PHYSICAL REVIEW A VOLUME 57, NUMBER 3 MARCH 1998

Lasing without inversion in three-level systems: Self-pulsing in the cascade schemes

J. Mompart,* C. Peters, and R. Corbalán
Departament de Física, Universitat Autònoma de Barcelona, E-08193 Bellaterra, Spain
(Received 28 January 1997; revised manuscript received 27 October 1997)

Lasing without inversion (LWI) in specific models of closed three-level systems is analyzed in terms of nonlinear dynamics. From a linear stability analysis of the trivial nonlasing solution of the homogeneously broadened systems with on-resonance driving and laser fields, we find that, near lasing threshold, resonant closed Λ and V schemes yield continuous-wave LWI while resonant cascade schemes can give rise to self-pulsing LWI. The origin of this different behavior is discussed. For parameters of a real cascade system in atomic ^{138}Ba we check numerically that the self-pulsing solution is stable in a broad range of nonzero detunings. It is shown that the self-pulsing emission can still be observed when the typical residual Doppler broadening of an atomic beam is taken into account. [S1050-2947(98)06803-6]

PACS number(s): 42.50.Gy, 32.80.Qk, 42.65.Vh

I. INTRODUCTION

In recent years, lasing (LWI) and amplification (AWI) without inversion have been discussed in many of the possible three- and four-level schemes. Recently, Sanchez-Morcillo *et al.* applied the techniques of nonlinear dynamics to the analysis of LWI considering explicitly the generation of the coherent laser field in a cavity [1]. They found that LWI based on a three-level system with a continuous-wave (cw) driving field can, in principle, show self-pulsing emission. Nevertheless, with their very general treatment of the necessarily involved incoherent processes it was impossible to predict the behavior of the different three-level systems of Fig. 1 as a function of the parameters which can be controlled experimentally.

We adopt the theoretical treatment of [1], but introduce the incoherent processes in the usual explicit manner, which allows us to demonstrate a fundamental difference between the closed three-level systems shown in Fig. 1 with on-resonance driving and laser fields: near lasing threshold, Λ and V systems generate cw laser light, whereas the cascade systems can lead to self-pulsing emission. The origin of this different behavior of the resonantly driven folded and cascade schemes is to be traced back to the fact, shown by Mandel and Kocharovskaya [2], that, with the incoherent pumping and relaxation schemes assumed here (see Fig. 1), AWI arises either at line center in the closed folded schemes, or at two symmetrical sidebands placed outside the absorbing Rabi sidebands in the closed cascade schemes [2]. We show that the simultaneous amplification of these two symmetrical sidebands gives rise to a periodically modulated laser output at the probe transition frequency. It is well known [3] that lasers in which two fields can be simultaneously amplified can exhibit also asymmetric emission regimes for which the two generated fields have different intensities, even in the fully symmetric case. We focus here on the self-pulsing LWI regime and have identified numerically a domain of parameters for a real cascade system in atomic ^{138}Ba where the self-pulsing solution is stable. Including the Doppler broadening for the cascade system in the barium atom, we find that the self-pulsing emission should be observable in an atomic beam experiment.

After submission of this paper we became aware of a systematic study of nonlinear dynamics in homogeneously broadened single mode three-level lasers without inversion, where the general case with cavity and driving field detunings is considered [4]. The analysis of the resonant case in that study confirms our main conclusion that, with incoherent relaxation and pumping processes as in Fig. 1, only the cascade schemes can exhibit stable self-pulsing LWI near lasing threshold.

II. THREE-LEVEL MODELS

We consider the four closed three-level schemes shown in Fig. 1. In all schemes, a coherent driving field $\mathbf{E}_\beta$ with Rabi frequency 2β interacts with a transition labeled 3-2 and prepares the atoms in order to generate a laser field $\mathbf{E}_\alpha$ with Rabi frequency 2α in a ring laser cavity. In addition, the upper level of the lasing transition is populated by an inco-

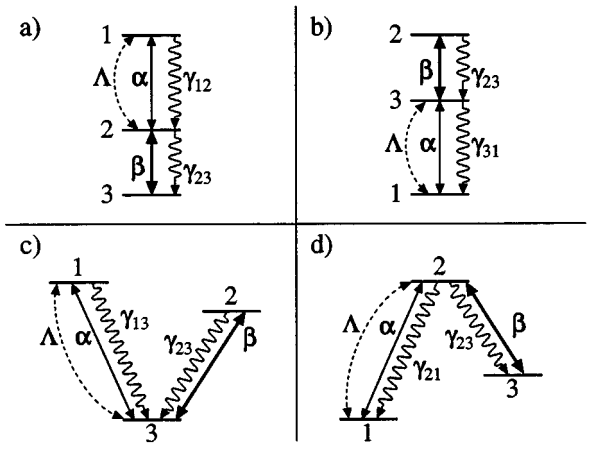

FIG. 1. The considered level schemes: (a) cascade scheme with the driving field in the lower transition, (b) cascade scheme with the driving field in the upper transition, (c) V scheme, (d) Λ scheme.

*Fax number: (34)-3-581 2155. Electronic address: ifop0@cc.uab.es

herent pump process interacting with this transition and represented by a rate Λ.

From the nonlinear dynamics point of view, a lasing solution corresponds to the destabilization of the trivial solution of the Maxwell-Schrödinger equations with the electric field amplitude α equal to zero. Thus we calculate this solution and perform a linear stability analysis.

A. Cascade schemes

In the following, we will discuss explicitly the cascade configuration of Fig. 1(a) with both coherent fields and the laser cavity on resonance with the corresponding transition. In the framework of the semiclassical theory and using the standard density matrix formalism with the rotating wave and slowly varying envelope approximation, the Maxwell-Schrödinger equations of this scheme can be written as

$$\dot{\rho}_{11}=-\gamma_{12}\rho_{11}+\Lambda(\rho_{22}-\rho_{11})+i[\alpha\rho_{12}^{*}-\text{c.c.}], \tag{1a}$$

$$\dot{\rho}_{22}=-\gamma_{23}\rho_{22}+\gamma_{12}\rho_{11}+\Lambda(\rho_{11}-\rho_{22})+i[\beta\rho_{23}^{*}+\alpha^{*}\rho_{12}-\text{c.c.}], \tag{1b}$$

$$\dot{\rho}_{33}=\gamma_{23}\rho_{22}-i[\beta\rho_{23}^{*}-\text{c.c.}], \tag{1c}$$

$$\dot{\rho}_{12}=-\Gamma_{12}\rho_{12}+i[\alpha(\rho_{22}-\rho_{11})-\beta^{*}\rho_{13}], \tag{1d}$$

$$\dot{\rho}_{23}=-\Gamma_{23}\rho_{23}+i[\beta(\rho_{33}-\rho_{22})+\alpha^{*}\rho_{13}], \tag{1e}$$

$$\dot{\rho}_{13}=-\Gamma_{13}\rho_{13}+i[\alpha\rho_{23}-\beta\rho_{12}], \tag{1f}$$

$$\dot{\alpha}=-\kappa\alpha+ig\rho_{12}, \tag{1g}$$

with $\rho_{11}+\rho_{22}+\rho_{33}=1$. κ designates the damping rate of the lasing field $\mathbf{E}_{\alpha}$ due to cavity losses and $g=\pi\nu_{\alpha}N\mu_{\alpha}^{2}/(\hbar\varepsilon_{0})$ the unsaturated gain of the lasing transition. ν_{α} is the corresponding transition frequency, μ_{α} the dipole matrix element, N the density of atoms, $\hbar$ Planck's constant, and ε_{0} the dielectric permittivity. The decay rates γ_{12} and γ_{23} describe phenomenologically the spontaneous relaxation of driving and lasing transitions. Depletion of the driving field is neglected. In the radiative limit, the decay rates of the coherences are given by

$$\Gamma_{12}=\frac{1}{2}(\gamma_{12}+\gamma_{23}+2\Lambda), \tag{2a}$$

$$\Gamma_{23}=\frac{1}{2}(\gamma_{23}+\Lambda), \tag{2b}$$

$$\Gamma_{13}=\frac{1}{2}(\gamma_{12}+\Lambda). \tag{2c}$$

In resonance, it is possible to take $\alpha=\alpha^{*}$, $\beta=\beta^{*}$ and the coherences can be expressed as $\rho_{12}\equiv iy_{12}$, $\rho_{23}\equiv iy_{23}$, and $\rho_{13}\equiv x_{13}$ with the real variables y_{12}, y_{23}, and x_{13} [5]. In our notation, $\alpha y_{12}>0$ (<0) and $\beta y_{23}>0$ (<0) lead to absorption (amplification) of the corresponding field.

Taking $\alpha=0$ (and thus $\rho_{12}=\rho_{13}=0$) and all time derivatives in Eqs. (1) equal to zero, the nonlasing solution is

$$\rho_{11}=\frac{4\Lambda\beta^{2}}{A}, \tag{3a}$$

$$\rho_{22}=\frac{4(\gamma_{12}+\Lambda)\beta^{2}}{A}, \tag{3b}$$

$$\rho_{33}=\frac{(\gamma_{12}+\Lambda)[\gamma_{23}(\gamma_{23}+\Lambda)+4\beta^{2}]}{A}, \tag{3c}$$

$$y_{23}=\frac{2\gamma_{23}(\gamma_{12}+\Lambda)\beta}{A}, \tag{3d}$$

with

$$A=\gamma_{23}(\gamma_{12}+\Lambda)(\gamma_{23}+\Lambda)+4(2\gamma_{12}+3\Lambda)\beta^{2}. \tag{3e}$$

Clearly, neither of both transitions is inverted, and, since $\beta y_{23}>0$, the driving field is absorbed.

The stability of the nonlasing solution is governed by a 7×7 matrix which splits into two independent submatrices. One of them governs the stability of the variables α, y_{12}, and x_{13} and therefore the generation of the lasing field. The characteristic polynomial of this submatrix is

$$\lambda^{3}+c_{1}\lambda^{2}+c_{2}\lambda+c_{3}=0, \tag{4}$$

with the coefficients

$$c_{1}=\Gamma_{12}+\Gamma_{13}+\kappa, \tag{5a}$$

$$c_{2}=\kappa(\Gamma_{12}+\Gamma_{13})+\Gamma_{12}\Gamma_{13}+\beta^{2}+gn_{21}, \tag{5b}$$

$$c_{3}=\kappa(\Gamma_{12}\Gamma_{13}+\beta^{2})+g(\Gamma_{13}n_{21}+\beta y_{23}), \tag{5c}$$

where $n_{21}\equiv\rho_{22}-\rho_{11}$. We apply the Hurwitz criteria for determining the instabilities associated with the above polynomial: c_{1}, c_{2}, $c_{3}>0$ and $H_{2}\equiv c_{1}c_{2}-c_{3}>0$ signify negative real parts of all eigenvalues which means stability of the nonlasing solution. The destabilization of the trivial solution occurs through a pitchfork bifurcation (static instability) if $c_{3}<0$ or, alternatively, through a Hopf bifurcation (self-pulsing instability) if $H_{2}<0$. In this case, $\sqrt{c_{2}}$ gives the angular pulsation frequency of $\mathbf{E}_{\alpha}$ at the destabilization point. Here, H_{2} is

$$H_{2}=(\Gamma_{12}+\Gamma_{13})[\kappa(\kappa+\Gamma_{12}+\Gamma_{13})+\Gamma_{12}\Gamma_{13}+\beta^{2}]+g[(\Gamma_{12}+\kappa)n_{21}-\beta y_{23}]. \tag{5d}$$

As $n_{21}>0$, the only term that can contribute to the destabilization of the nonlasing solution is βy_{23}. It follows from Eq. (3) that the driving field is absorbed ($\beta y_{23}>0$) and, consequently, the destabilization of the nonlasing solution can occur only via a Hopf bifurcation which gives rise to self-pulsing laser emission. For $\beta=0$ as well as for very large values of β^{2}, H_{2} is positive and the nonlasing solution is stable. Varying the driving field intensity β^{2}, there are consequently two ways to obtain the destabilization of the nonlasing solution: increasing β^{2} starting with a very small value or, alternatively, decreasing β^{2} from a very large value. It should be emphasized that a direct calculation of the probe field amplification without cavity as it has been carried

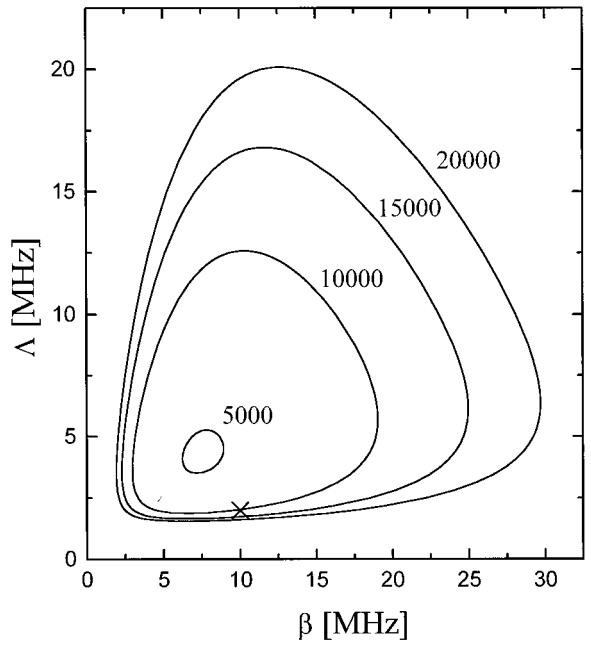

FIG. 2. LWI regions in the plane of parameters β and Λ for various values of the gain parameter g. The values of g are given in MHz^2. The other parameters are $\gamma_{12}=3.5$, $\gamma_{23}=19$, and $\kappa=0.5$ (all in MHz).

out in [6–8] leads to steady-state probe field absorption when probe and driving fields are taken on resonance. This demonstrates the difference between AWI and LWI in the cascade schemes.

Substituting the nonlasing stationary solution (3) into Eq. (5d), it is easily seen that the inequality

$$\gamma_{23} > 2\gamma_{12} \tag{6}$$

is a necessary condition for LWI. This means that the spontaneous decay rate of the driving field transition has to be at least twice that of the lasing transition. The threshold values of all parameters can be obtained analytically from condition $H_2<0$. For example, the threshold value of the incoherent pump rate Λ is given by

$$\Lambda > \gamma_{12}\frac{\gamma_{12}+2\kappa}{\gamma_{23}-2\gamma_{12}} + o\left(\frac{1}{g}\right). \tag{7}$$

The threshold values for all schemes of Fig. 1 will be discussed elsewhere.

Figure 2 shows different curves $H_2=0$ as a function of the parameters β and Λ for different values of the gain parameter g [9]. For a given gain, LWI is obtained within a closed curve in the β-Λ plane ($H_2<0$). Outside this curve the nonlasing solution is stable. The cross marks the values of β and Λ which are used in Figs. 3 and 4. We choose a Λ value just above threshold since the realization of an efficient incoherent pump represents the main difficulty in AWI and LWI experiments.

Figures 3(a) and 3(b) represent the results of a numerical integration of Eqs. (1) using a seventh- to eighth-order Runge-Kutta-Fehlberg routine. The parameters are $\beta=10$ MHz, $\Lambda=2$ MHz, and $g=15\,000$ MHz^2 with γ_{12}, γ_{23}, and

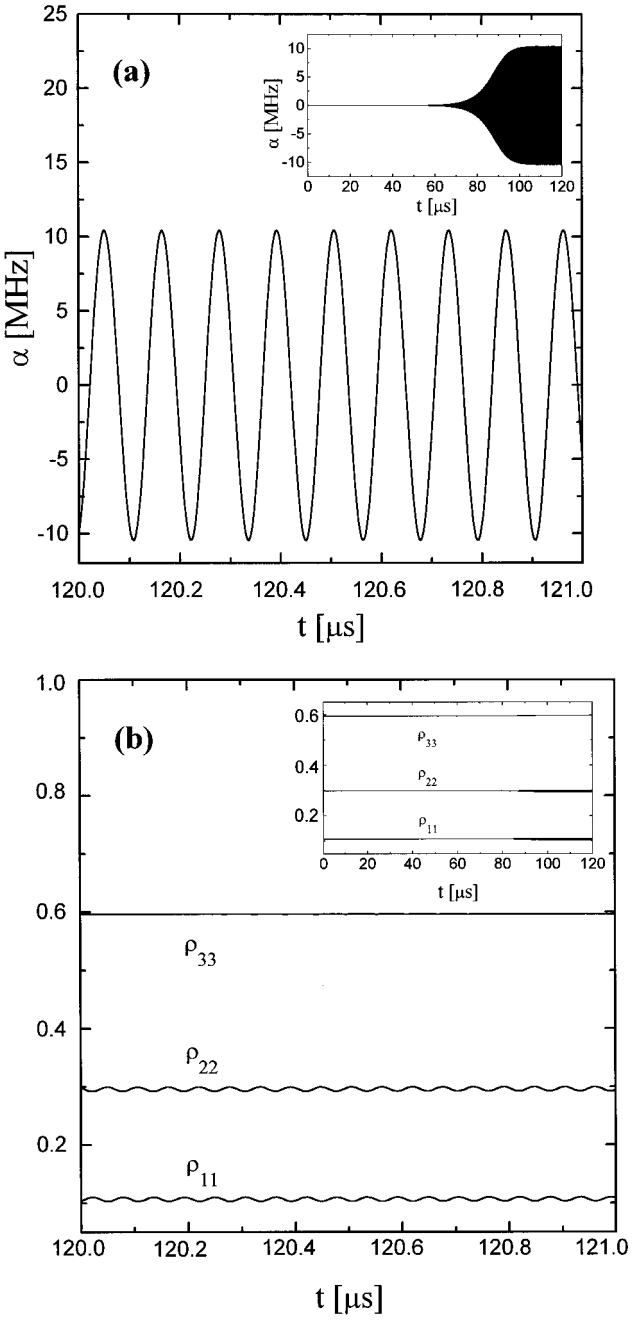

FIG. 3. (a) Evolution of the laser field amplitude, (b) corresponding evolution of the atomic populations. The parameters are given in the text.

κ as in Fig. 2. After a transient which is shown in the insets, the laser field amplitude $\mathbf{E}_\alpha$ oscillates symmetrically around zero with an angular frequency $2\pi(8.75)=55$ MHz, while the populations oscillate with very small amplitudes, and neither of the transitions is inverted. A numerical study of AWI for the parameters of Fig. 3 shows that the maxima in amplification of the additional sidebands appear for probe field detunings $\Delta_\alpha=\pm 55$ MHz. This shows that the self-pulsing emission at line center is due to the simultaneous amplification of these two additional sidebands. Since we have considered thus far a resonant laser field, Eqs. (1) do not admit solutions with time-independent intensity, corresponding to the amplification of only one of the (detuned) sidebands.

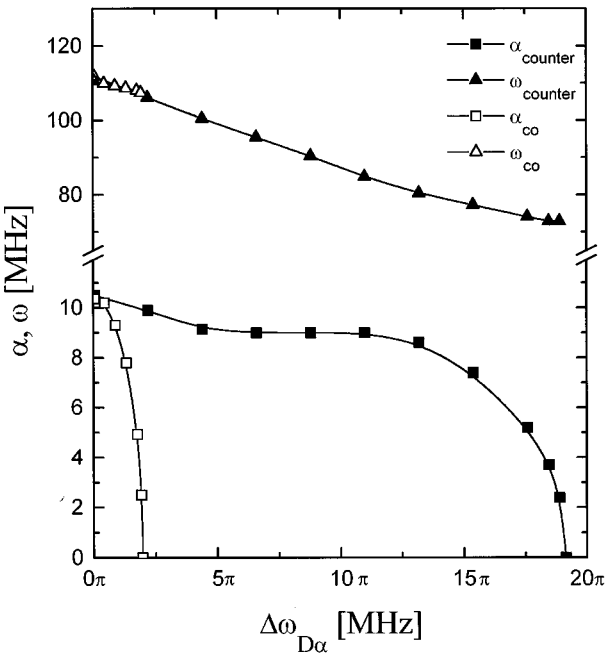

FIG. 4. Maximal laser field strength $\sqrt{e^2+f^2}$ of the self-pulsing after the transient and pulsation frequency ω of this quantity as a function of the Doppler broadening $\Delta\omega_{D\alpha}$. The parameters are the same as in Fig. 3.

Therefore these equations do not allow us to investigate whether the self-pulsing state emerging from the Hopf bifurcation is stable or unstable. This issue is studied analytically in Ref. [4]. Instead, we have checked numerically that, for the conditions of Fig. 1(a), this self-pulsing state is stable. For this purpose we considered a full set of equations analogous to Eqs. (1), but including both cavity and driving field detunings Δ_α and Δ_β, respectively [see Eq. (14) below]. We studied first the laser behavior as a function of Δ_α, with $\Delta_\beta=0.1$ MHz and other parameters as in Fig. 3. For various cavity detunings up to $\Delta_\alpha\simeq 15$ MHz we obtained stable self-pulsing emission, with both the maximum generated field intensity and the modulation depth decreasing with increasing cavity detuning. In all cases the intensity pulsing frequency was, as in resonance, 110 MHz. For $\Delta_\alpha>15$ MHz we obtained cw emission. A similar behavior was observed when the cavity detuning was kept fixed at $\Delta_\alpha=0.1$ MHz and the driving field detuning Δ_β was varied, except that we obtained self-pulsing emission up to $\Delta_\beta\simeq 0.7$ MHz and a cw regime for $\Delta_\beta>0.7$ MHz. The system is therefore more sensitive to driving field detuning, which breaks the symmetry between the two amplifying sidebands, than to cavity detuning [4]. We have checked numerically that it is possible to increase the cavity and driving detuning domain for which the self-pulsing regime is stable by increasing the unsaturated gain parameter or, alternatively, by decreasing the cavity losses.

For the cascade scheme of Fig. 1(b) the results are similar. Again, the only way to destabilize the nonlasing solution is through a Hopf bifurcation giving rise to self-pulsing LWI emission with the necessary condition $\gamma_{23}>2\gamma_{31}$. In the same way as for the other cascade scheme, we have checked numerically that there is also a broad domain of parameters where the self-pulsing solution is stable.

It is well known that a conventional incoherently pumped laser without driving field can show self-pulsing and even chaotic emission if the gain of the lasing transition and the cavity losses are sufficiently large [10]. This dynamical behavior corresponds to a destabilization of a cw lasing solution while the destabilization of the nonlasing solution occurs always through a pitchfork bifurcation leading primarily to cw output. In contrast, the self-pulsing output of the cascade schemes is obtained directly through a destabilization of the nonlasing solution. Furthermore, the self-pulsing appears even without cavity losses.

It should be mentioned that in Ref. [11] cw laser emission has been observed experimentally in a closed cascade system. However, a comparison with our results is not possible since in this experiment the incoherent pump process was substituted by a second coherent driving field with the same frequency as the laser field.

B. Folded schemes

For the folded schemes the procedure is analogous, and the destabilization of the trivial solution is again governed by a 3×3 matrix. For the V-type system of Fig. 1(c), the coefficients of the characteristic polynomial are

$$c_1=\kappa+\Gamma_{12}+\Gamma_{13}, \tag{8a}$$

$$c_2=\kappa(\Gamma_{12}+\Gamma_{13})+\Gamma_{12}\Gamma_{13}+\beta^2+gn_{31}, \tag{8b}$$

$$c_3=\kappa(\Gamma_{12}\Gamma_{13}+\beta^2)+g(\Gamma_{12}n_{31}-\beta y_{23}), \tag{8c}$$

$$H_2=(\Gamma_{12}+\Gamma_{13})[\kappa(\kappa+\Gamma_{12}+\Gamma_{13})+\Gamma_{12}\Gamma_{13}+\beta^2] +g[(\Gamma_{13}+\kappa)n_{31}+\beta y_{23}], \tag{8d}$$

with $n_{31}=\rho_{33}-\rho_{11}$, and for the Λ-type system of Fig. 1(d)

$$c_1=\kappa+\Gamma_{12}+\Gamma_{13}, \tag{9a}$$

$$c_2=\kappa(\Gamma_{12}+\Gamma_{13})+\Gamma_{12}\Gamma_{13}+\beta^2+gn_{12}, \tag{9b}$$

$$c_3=\kappa(\Gamma_{12}\Gamma_{13}+\beta^2)+g(\Gamma_{12}n_{12}-\beta y_{23}), \tag{9c}$$

$$H_2=(\Gamma_{12}+\Gamma_{13})[\kappa(\kappa+\Gamma_{12}+\Gamma_{13})+\Gamma_{12}\Gamma_{13}+\beta^2] +g[(\Gamma_{12}+\kappa)n_{12}+\beta y_{23}], \tag{9d}$$

with $n_{12}=\rho_{11}-\rho_{22}$. As expected, in the limit $\beta\to 0$ the stability condition is fulfilled. From the Maxwell-Schrödinger equations it is easy to verify that in both cases the lasing transition is not inverted, i.e., $n_{31}>0$ for the V-type system and $n_{12}>0$ for the Λ-type system. Furthermore, the driving field is again absorbed, i.e., $\beta y_{23}>0$. Consequently, the only way to destabilize the nonlasing solution is now via a pitchfork bifurcation which gives rise to continuous wave LWI. This is consistent with the result [2] that closed folded schemes driven in resonance show AWI at line center. Necessary conditions for $c_3<0$ are now

$$\gamma_{23}>\gamma_{13}\ \ (V\ \text{scheme}) \text{ and } \gamma_{23}>\gamma_{12}\ \ (\Lambda\ \text{scheme}). \tag{10}$$

In the high gain limit, this bifurcation occurs in the V-type system for

$$\frac{\beta y_{23}}{\Gamma_{12}} > n_{31}. \tag{11}$$

The usual discussion of continuous-wave amplification without inversion (AWI) in the V scheme leads to the amplification condition [12]

$$-y_{13} > 2\frac{\alpha n_{13} + \beta x_{12}}{\gamma_{13} + 2\Lambda}, \tag{12}$$

which involves directly the real part of the two-photon coherence x_{12}, and AWI is explained as due to the contribution of this coherence. In contrast, the lasing condition (11) for LWI does not involve x_{12}. At the destabilization point of the nonlasing solution we have $x_{12} \approx 0$. Consequently, following Eq. (12) one can think naïvely that, at least at the destabilization point, population inversion is required to achieve amplification. It is important to remark that at the bifurcation point Eq. (12) does not hold and should be substituted by Eq. (11), which has been obtained through a nonlinear dynamical analysis that allows us to characterize the bifurcation. On the other hand, in the limit $\Gamma_{12} \to \infty$, where the two-photon coherence could not be generated, Eq. (11) indicates that LWI is not possible. This shows that this coherence is also essential for LWI.

In order to realize frequency up conversion with the closed three-level schemes, the frequency of the lasing transition must be larger than the frequency of the driving transition 3-2. Due to the scaling of the spontaneous emission probability with the cube of the transition frequency, it is difficult to find three-level systems in real atoms which fulfill the conditions (6) or (10) and permit at the same time frequency up conversion. A possibility could be to use dipole-forbidden laser transitions (i.e., metastable levels).

III. DOPPLER BROADENING

In order to investigate if the self-pulsing emission of the cascade schemes will be observable experimentally, it has to be taken into account that experiments are made with free atoms. Atomic motion leads unavoidably to Doppler broadening and can change significantly the atom-light interaction. Typical values of the Doppler broadening at optical frequencies are 1 GHz for a vapor cell, a few MHz for a collimated atomic beam, and a few hundred kHz for an atomic trap. The influence of the Doppler broadening on cw LWI has been discussed in [13] for Λ and V schemes and in [8] for the cascade schemes.

The Doppler effect leads to a velocity-dependent shift $\Delta_{\alpha,\beta}$ of the cavity and driving field frequencies with respect to the atomic transition frequencies: $\omega_{\alpha,\beta}(v_z) = \omega_{\alpha,\beta}(v_z = 0) + \Delta_{\alpha,\beta}(v_z) = \omega_{\alpha,\beta}(v_z = 0)(1 \pm v_z/c)$. v_z designates the atom velocity component parallel to the direction of the light, c the velocity of the light. For the atomic velocities, we assume a Maxwell-Boltzmann distribution

$$\rho(v_z) = \frac{1}{v_{zp}\sqrt{\pi}} \exp(-v_z^2/v_{zp}^2), \tag{13}$$

with the most probable velocity v_{zp}. The Doppler broadenings (full width at half maximum) are then given by $\Delta\omega_{D\alpha,\beta} \equiv 2\Delta_{\alpha,\beta}(v_{zp})\ln(2)$ with $\Delta\omega_{D\beta} = (\lambda_\alpha/\lambda_\beta)\Delta\omega_{D\alpha}$.

The laser field $\mathbf{E}_\alpha$ is generated by all atoms. If the cavity is resonant with the frequency $\omega_\alpha(v_z = 0)$, $\mathbf{E}_\alpha$ will also be in resonance. To simulate the generation of $\mathbf{E}_\alpha$, we consider n_v velocity classes, each of them with the corresponding transition frequencies $\omega_\alpha(v_z)$ and $\omega_\beta(v_z)$ and with a set of equations such as Eqs. (1a)–(1f), but with the equations of the coherences being now

$$\begin{aligned}
\dot{\rho}_{12}^j &= -(\Gamma_{12} - i\Delta_\alpha^j)\rho_{12}^j + i[\alpha(\rho_{22}^j - \rho_{11}^j) - \beta^*\rho_{13}^j], \\
\dot{\rho}_{23}^j &= -(\Gamma_{23} - i\Delta_\beta^j)\rho_{23}^j + i[\beta(\rho_{33}^j - \rho_{22}^j) + \alpha^*\rho_{13}^j], \\
\dot{\rho}_{13}^j &= -(\Gamma_{13} - i[\Delta_\alpha^j + \Delta_\beta^j])\rho_{13}^j + i[\alpha\rho_{23}^j - \beta\rho_{12}^j].
\end{aligned} \tag{14}$$

The index j numbers the atomic velocity classes. The differential equation for $\mathbf{E}_\alpha$, Eq. (1g), becomes

$$\dot{\alpha} = -\kappa\alpha + ig\sum_{v_z} \rho_{12}(v_z). \tag{15}$$

Since α is now a complex number, $\alpha \equiv e + if$, the total number of real equations becomes $9n_v + 2$. The Maxwell-Boltzmann distribution is included in the initial conditions of the atomic populations. In the calculations presented in Fig. 4, we have used $n_v = 40$. Different initial values for e and f yielded the same final results. It is assured that further increasing of n_v does not change the results.

For the simulation of the Doppler broadening, we choose the parameters of a real cascade system in atomic ^{138}Ba which has already been used experimentally by Sellin *et al.* [11]. The wavelengths of the atomic transitions are $\lambda_\alpha = 821$ nm and $\lambda_\beta = 554$ nm, the corresponding decay rates $\gamma_{12} = 3.5$ MHz and $\gamma_{23} = 19$ MHz. Thus the system works with frequency down conversion, nevertheless it allows the observation of the self-pulsing emission. Figure 4 shows the results of our calculations with a Runge-Kutta-Fehlberg routine of order 7 to 8, the other parameters have the same values as in Fig. 3. We represent the maxima of the laser field strength $|\alpha| = \sqrt{e^2 + f^2}$ within the cavity and the self-pulsing frequency ω of the laser field intensity as a function of the Doppler broadening $\Delta\omega_{D\alpha}$. As has already been discussed for AWI, counterpropagating coherent fields are more favorable for the cascade systems while copropagating fields are more favorable for Λ and V systems [13,8]. With counterpropagating fields, laser output can be observed up to $\Delta\omega_{D\alpha} = 20\pi$ MHz which is much more than the typical value for a collimated atomic beam. Thus the self-pulsing should be observable in laser-cooled or atomic beam experiments, whereas the use of gas or vapor cells would hinder laser oscillations.

IV. CONCLUSIONS

We have analyzed the inversionless generation of a laser field in a resonant cavity, the active medium consisting of specific models of closed three-level atoms in different configurations driven in resonance with a continuous wave. While the closed Λ and V systems lead to cw laser emission

near lasing threshold, the closed cascade schemes can generate self-pulsing laser output. The origin of this different behavior lies in the fact, shown by Mandel and Kocharovskaya [2], that while AWI arises in closed folded schemes at line center, it arises only at the sidebands for the closed cascade schemes. Our analysis proves that a simple calculation of the steady-state amplification (AWI) is not sufficient to predict LWI. It should be emphasized that for on-resonance probe and driving fields in the closed cascade schemes, a laser analysis leads to self-pulsing LWI emission while a gain analysis without taking into account the laser cavity leads to steady-state probe absorption. In contrast to conventional lasers, the self-pulsing emission of the cascade schemes results directly from a destabilization of the trivial nonlasing solution and occurs even without cavity losses. We have probed numerically that for the closed cascade schemes shown in Figs. 1(a) and 1(b), the self-pulsing emission is stable. Numerical calculations reveal that the Doppler broadening decreases the laser intensity as well as the self-pulsing frequency. Nevertheless, the self-pulsing should be observable under the typical conditions of an atomic beam experiment.

An analysis analogous to the one in this paper shows that LWI based on a double-Λ system can generate both cw and self-pulsing emission depending on the parameter values [14]. The underlying mechanism involves also the coherent population trapping, and the pulsed emission has an origin similar to that in a conventional laser with large gain and cavity losses.

ACKNOWLEDGMENTS

We thank Paul Mandel for sending us results prior to publication and M. D. Lukin for useful discussion on self-pulsing LWI. We acknowledge support from the DGICYT (Spanish Government) under Contract No. PB95-0778-C02-02. J.M. acknowledges support from the DGICYT for Grant No. FP94-38105342. C.P. acknowledges support from the Human Capital and Mobility Program, Access to Large Installations, under Contract No. CHGE-CT92-0009 established between the European Community and CESCA/CEPBA.

[1] V. Sanchez-Morcillo, E. Roldán, and G. J. de Valcárcel, Quantum Semiclassic. Opt. **7**, 889 (1995).
[2] P. Mandel and O. Kocharovskaya, Phys. Rev. A **46**, 2700 (1992).
[3] See, for instance, M. Sargent III, M. O. Scully, and W. E. Lamb, Jr., *Laser Physics* (Addison-Wesley, Reading, MA, 1974), pp. 120–127; E. Roldán, G. J. de Valcárcel, R. Vilaseca, and V. Espinosa, J. Mod. Opt. **44**, 83 (1997).
[4] A. G. Vladimirov, P. Mandel, S. F. Yelin, M. D. Lukin, and M. O. Scully (unpublished).
[5] These simplifying assumptions facilitate the analytical study but exclude the possibility of detuned continuous-wave lasing without inversion in resonant closed cascade schemes. This possibility will be explored here numerically with a set of equations involving complex variables. See below in this section, discussion following Fig. 3. See also Ref. [4].
[6] O. Kocharovskaya, P. Mandel, and Y. V. Radeonychev, Phys. Rev. A **45**, 1997 (1992).
[7] G. Vemuri and D. M. Wood, Phys. Rev. A **50**, 747 (1994).
[8] G. Vemuri and G. S. Agarwal, Phys. Rev. A **53**, 1060 (1996).
[9] All frequencies given in this paper are angular frequencies.
[10] L. M. Narducci and N. B. Abraham, *Laser Physics and Laser Instabilities* (World Scientific, Singapore, 1988).
[11] P. B. Sellin, G. A. Wilson, K. K. Meduri, and T. W. Mossberg, Phys. Rev. A **54**, 2402 (1996).
[12] Y. Zhu, Phys. Rev. A **45**, R6149 (1992).
[13] A. Karawajczyk and J. Zakrzewski, Phys. Rev. A **51**, 830 (1995).
[14] R. Corbalán, J. Mompart, R. Vilaseca, and E. Arimondo, Quantum Semiclassic. Opt. (to be published).